Electronic Supplementary Information

Threading of three rings on two stations: a convergent approach to [4]rotaxane

Yidan Zhou,‡[a] Jinyang Wu,‡[a] Zejiang Liu,[a] Weitao Xu,[b] Menglong Liu,[a] Along Jia,[a] Yuchen Liu,[a] Xin Xiao,[b] Xiaowei Li*[a] and Lihua Yuan*[a]

[a] *Sichuan University, Chengdu 610064, Sichuan, China. E-mail: lhyuan@scu.edu.cn, xiaoweili110889@163.com*

[b] *Key Laboratory of Macrocyclic and Supramolecular Chemistry of Guizhou Province, Guizhou University, Guiyang 550025, China*

‡These authors contributed equally to the work.

Contents

1. Materials and Methods

The ^{1}H NMR and ^{13}C NMR spectra were recorded on Bruker AVANCE AV II-400 MHz (^{1}H: 400 MHz, 600 MHz; ^{13}C: 100 MHz). $CDCl_3$ and CD_3CN were purchased from Cambridge Isotope Laboratories, and were used for the titration experiments without further drying. Chemical shifts are reported in δ values in ppm using tetramethylsilane (TMS) and coupling constants (J) are denoted in Hz. Multiplicities are denoted as follows: s = singlet, d = doublet, t = triplet, dd = double doublet, and m = multiplet. All chemicals were obtained from commercial suppliers and were used as received unless otherwise noted. CH_2Cl_2 was dried over CaH_2. Column chromatography was carried out using silica gel (300 - 400 mesh). Solvents for chromatography were reagent grade. ESI mass spectra were recorded on a Bruker Daltonics MicroTOF-Q II and Thermo Scientific Q Exactive hybrid quadrupole-Orbitrap mass spectrometer. UV-vis spectra were measured by SHIMADZU UV-2450. Binding constant were performed using an isothermal titration calorimeter Nano ITC (TA, USA). Single crystal X-ray data were measured on a Xcalibur E diffractometer with graphite monochromated Cu-Kα radiation (λ = 1.54184 Å). Data collection and structure refinement details can be found in the CIF files or obtained free of charge via www.ccdc.cam.ac.uk/.

2. Synthesis

2.1 Synthesis of Guests G1-G2 and Axle

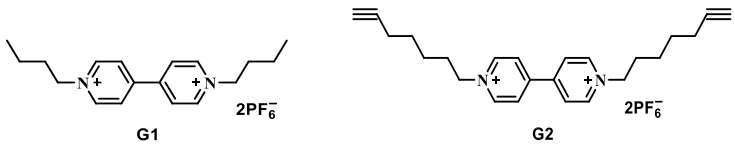

Guests **G1** and **G2** were prepared according to the similar procedures in the literature[1]

G1: ^{1}H NMR (400 MHz, CD_3CN, 298 K) δ 8.92 (d, *J* = 6.4 Hz, 4H), 8.40 (d, *J* = 6.4 Hz, 4H), 4.65 (t, *J* = 7.5 Hz, 4H), 2.07 - 1.99 (m, 4H), 1.49 - 1.40 (m, 4H), 1.02 (t, *J* = 7.4 Hz, 6H).

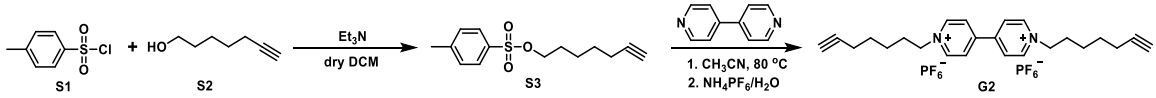

Scheme S1. Synthetic routes of the guest G2.

S3 was prepared according to the similar procedures in the literature[2]

S3: ^{1}H NMR (400 MHz, $CDCl_3$, 298 K) δ 7.79 (d, J = 8.0 Hz, 2H), 7.35 (d, J = 8.0 Hz, 2H), 4.03 (t, J = 6.4 Hz, 2H), 2.45 (s, 3H), 2.17 - 2.13 (m, 2H), 1.93 (t, J = 2.7 Hz, 1H), 1.70 - 1.63 (m, 2H), 1.51 - 1.37 (m, 4H).

G2: A mixture of neutral bipyridine (1.00 g, 6.40 mmol) and hept-6-yn-1-yl 4-methylbenzenesulfonate **S3** (6.82 g, 25.6 mmol) was stirred in 10 mL CH_3CN at 80 ℃ for 96 h, and then cooled to room temperature. The light yellow precipitate was filtered off and washed with CH_3CN (20 mL). The solid was then dissolved in H_2O (15 mL), and a saturated aqueous solution of NH_4PF_6 was added until no further precipitation was observed. The precipitate was filtered off and washed with H_2O (30 mL), EtOH (15 mL), and Et_2O (10 mL). Finally, it was recrystallized from Et_2O /CH_3CN to afford **G2** as a white solid (2.30 g, 56 %). ^{1}H NMR (400 MHz, CD_3CN, 298 K) δ 8.90 (d, *J* = 6.3 Hz, 4H), 8.38 (d, *J* = 6.3 Hz, 4H), 4.62 (t, *J* = 7.0 Hz, 4H), 2.24 - 2.20 (m, 4H), 2.08 - 2.00 (m, 4H), 2.18 (s, 2H), 1.62 - 1.55 (m, 4H), 1.53 - 1.45 (m, 4H). HRMS (ESI): m/z calcd for $[C_{24}H_{30}F_{12}N_2P_2 - 2PF_6]^{2+}$ 173.1199; found: 173.1198.

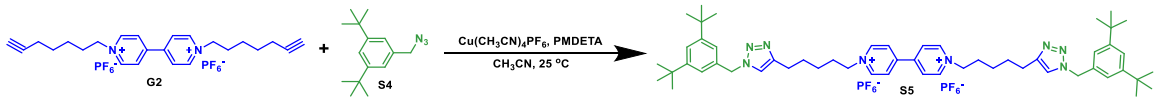

Scheme S2. Synthetic route of the S5.

S4 was prepared according to the similar procedures in the literature[1]

A mixture of guest **G2** (30 mg, 0.047 mmol) and 3,5-di-(tert-butyl)benzyl azide (**S4**) (34.7 mg, 0.15 mmol) was dissolved in dry CH_3CN (8 mL), and then $Cu(MeCN)_4PF_6$ (7 mg, 0.019 mmol) and PMDETA (3.3 mg, 0.019 mmol)was added under N_2. The brown solution was stirred at 25 °C for

24 h. The mixture was washed with CH_2Cl_2 /H_2O (2 × 20 mL) and the solvent was evaporated under reduced pressure. Then the crude material was purified by column chromatography using silica gel (eluent: CH_2Cl_2 and then CH_2Cl_2/MeOH (v/v)) and the main fraction was collected. The solid was dried under high vacuum to afford the **S5** as a dark brown solid (45 mg, 85 %). ^{1}H NMR (400 MHz, $CDCl_3$/CD_3CN, 1:1, v/v, 298 K) δ 8.93 (d, J = 6.4 Hz, 4H), 8.42 (d, J = 6.4 Hz, 4H), 7.50 (s, 2H), 7.40 (s, 2H), 7.14 (s, 4H), 5.45 (s, 4H), 4.63 (t, J = 7.5 Hz, 4H), 2.69 (t, J = 7.5 Hz, 4H), 2.12 - 2.04 (m, 4H), 1.77 - 1.70 (m, 4H), 1.51 - 1.41 (m, 4H), 1.29 (s, 36H). HRMS (ESI): m/z calcd for $[C_{54}H_{76}F_{12}N_8P_2 - 2PF_6]^{2+}$ 418.3091; found: 418.3084.

2.2 Synthesis of [4]rotaxane or [3]rotaxane

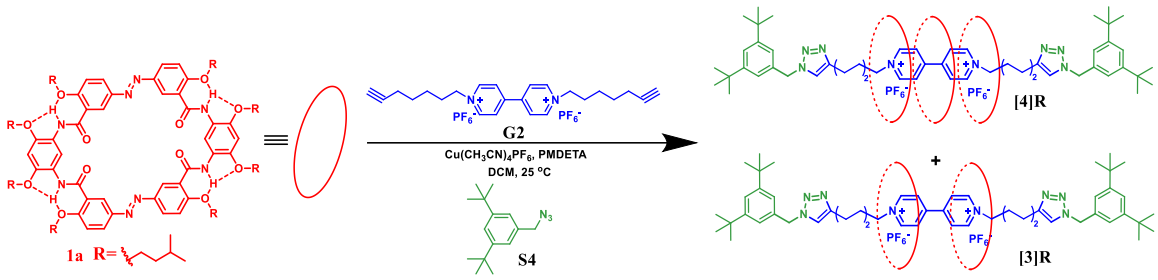

Scheme S3. Synthetic route of the Rotaxanes.

Macrocycle **1a** was prepared according to literature procedures.[3]

General procedure for [4]R

A mixture of macrocycle **1a** (108 mg, 0.079 mmol) and guest **G2** (5 mg, 0.008 mmol) and was stirred in dry CH_2Cl_2 (4 mL) at room temperature for 30 minutes under N_2. Then a solution (4 mL) of **S4** (3,5-di-tert-butylbenzyl azide, 5.8 mg, 0.024 mmol), $Cu(CH_3CN)_4PF_6$ (1.2 mg, 0.003 mmol) and N,N,N',N",N"-pentamethyl-diethylenetriamine (PMDETA) (1.1 mg, 0.006 mmol) was injected. The mixture was further stirred at 25 °C for 24 h. The resulting solution was washed with H_2O in the presence of EDTA to remove copper ion. The organic layer was retained and the aqueous layer extracted twice with CH_2Cl_2 (2 × 30 mL). Removal of solvents afforded a yellow solid and the crude material was purified by trituration using CH_3CN. The organic solvent was isolated, the solvent removed under reduced pressure to give **[4]R** as a yellow solid. (31 mg, 71%). ^{1}H NMR (400 MHz, $CDCl_3$/CD_3CN, 1:1, v/v, 298 K) δ 10.10 (d, J = 6.0 Hz, 4H), 9.98 (d, J = 6.0 Hz, 4H), 9.79 (s, 2H), 9.71 (d, J = 2.7 Hz, 4H), 9.40 (s, 8H), 9.11 (s, 4H), 8.14 (s, 8H), 7.50 (s, 4H), 7.41 (d, J = 5.5 Hz, 8H), 7.23 (d, J = 5.5 Hz, 4H), 7.16 (s, 2H), 6.77 (d, J = 9.3 Hz, 8H), 6.75 (s, 2H), 6.70 (s, 4H), 6.55 (d, J = 7.9 Hz, 4H), 6.45 (s, 4H), 6.28 (s, 2H), 5.17 (m, J = 7.8 Hz, 4H), 4.84 (s, 4H), 4.35 – 4.01 (m, 48H), 2.33 (m, J = 8.0 Hz, 4H), 1.92 - 1.70 (m, 80H), 1.45 - 1.36 (m, 4H), 1.24 - 1.00 (m, 180H). HRMS (ESI): m/z calcd for $[C_{294}H_{400}F_{12}N_{32}O_{36}P_2 + H - 2PF_6]^{3+}$ 1653.0205; found: 1653.0123, $[C_{294}H_{400}F_{12}N_{32}O_{36}P_2 + 2H - 2PF_6]^{4+}$ 1239.7664; found: 1239.7602.

General procedure for [3]R

A mixture of macrocycle **1a** (54.0 mg, 0.039 mmol) and guest **G2** (25 mg, 0.039 mmol) and was stirred in dry CH_2Cl_2 (4 mL) at room temperature for 30 minutes under N_2. Then a solution (4 mL) of **S4** (3,5-di-tert-butylbenzyl azide, 28.9 mg, 0.12 mmol), $Cu(CH_3CN)_4PF_6$ (5.9 mg, 0.016 mmol)

and N,N,N',N",N"-pentamethyl-diethylenetriamine (PMDETA) (5.4 mg, 0.031 mmol) was injected. The mixture was further stirred at 25 °C for 24 h. The resulting solution was washed with aqueous EDTA tetra-sodium saturated ammonia solution (2 × 20 mL). The organic layer was retained and the aqueous layer extracted twice with CH_2Cl_2 (2 × 30 mL). Removal of solvents afforded a yellow solid and the crude material was purified by flash column chromatography using silica gel (CH_2Cl_2/MeOH, 40:1, v/v) to give **[3]R** as a yellow solid (46 mg, 60 %). ^{1}H NMR (400 MHz, $CDCl_3$/CD_3CN, 1:1, v/v, 298 K) δ 9.98 (d, J = 6.4 Hz, 4H), 9.83 (s, 4H), 9.68 (d, J = 6.4 Hz, 4H), 9.61 (s, 8H), 8.10 (s, 8H), 7.60 (d, J = 8.6 Hz, 8H), 7.28 (s, 2H), 6.97 (s, 2H), 6.94 (s, 4H), 6.91 (d, J = 8.6 Hz, 8H), 6.57 (s, 4H), 5.18 (s, 4H), 4.64 (t, J = 7.2 Hz, 4H), 4.34 – 4.17 (m, 32H), 2.04 (t, J = 6.9 Hz, 5H), 1.94 – 1.74 (m, 50H), 1.32 – 1.24 (m, 4H), 1.16 (s, 36H), 1.15 – 0.69 (m, 112H). HRMS (ESI): m/z calcd for $[C_{294}H_{400}F_{12}N_{32}O_{36}P_2 + H - 2PF_6]^{3+}$ 1195.0832; found: 1195.0785.

3. Spectroscopic Characterization

3.1 ^{1}H and ^{13}C NMR Spectra of Novel Compounds

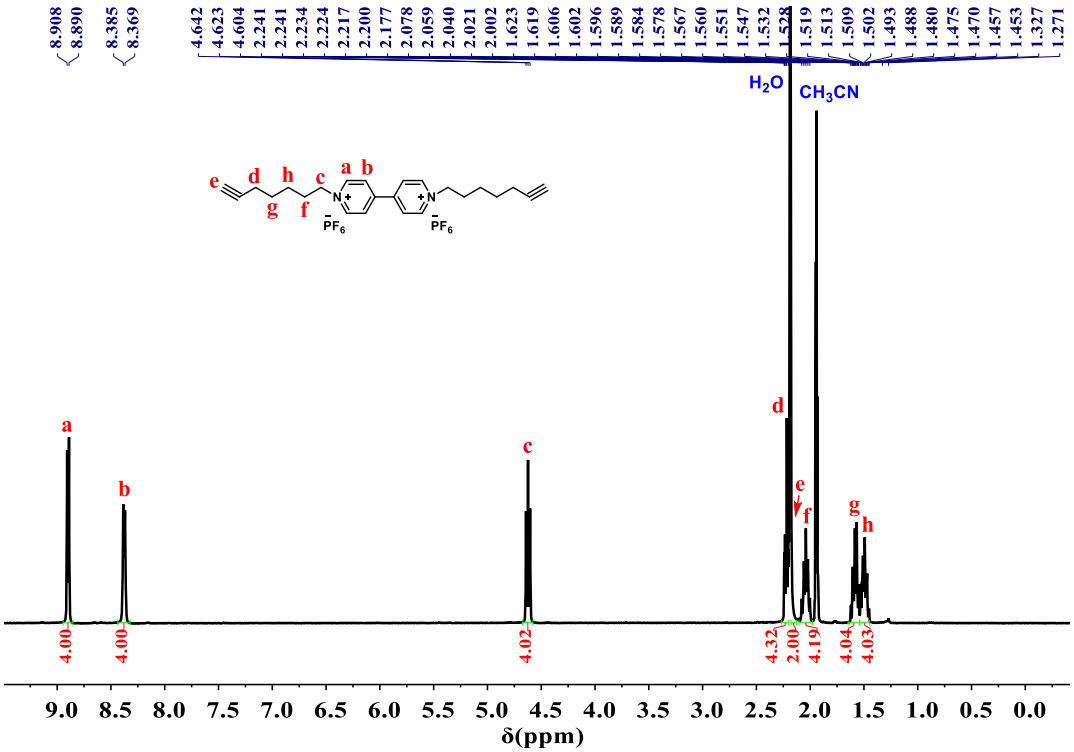

Figure S1 ^{1}H NMR spectrum of **G2** (400 MHz, CD_3CN , 298 K, 5 mM).

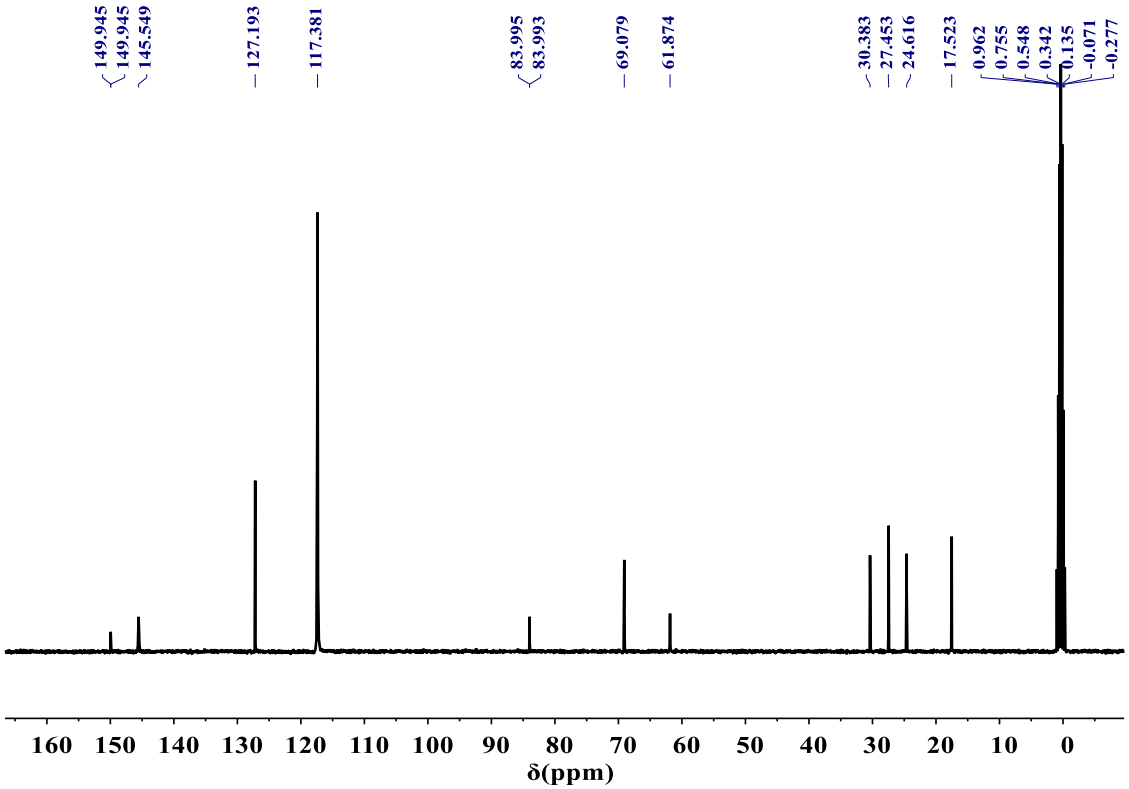

Figure S2 ^{13}C NMR spectrum of **G2** (100 MHz, CD_3CN, 298 K, 15 mM).

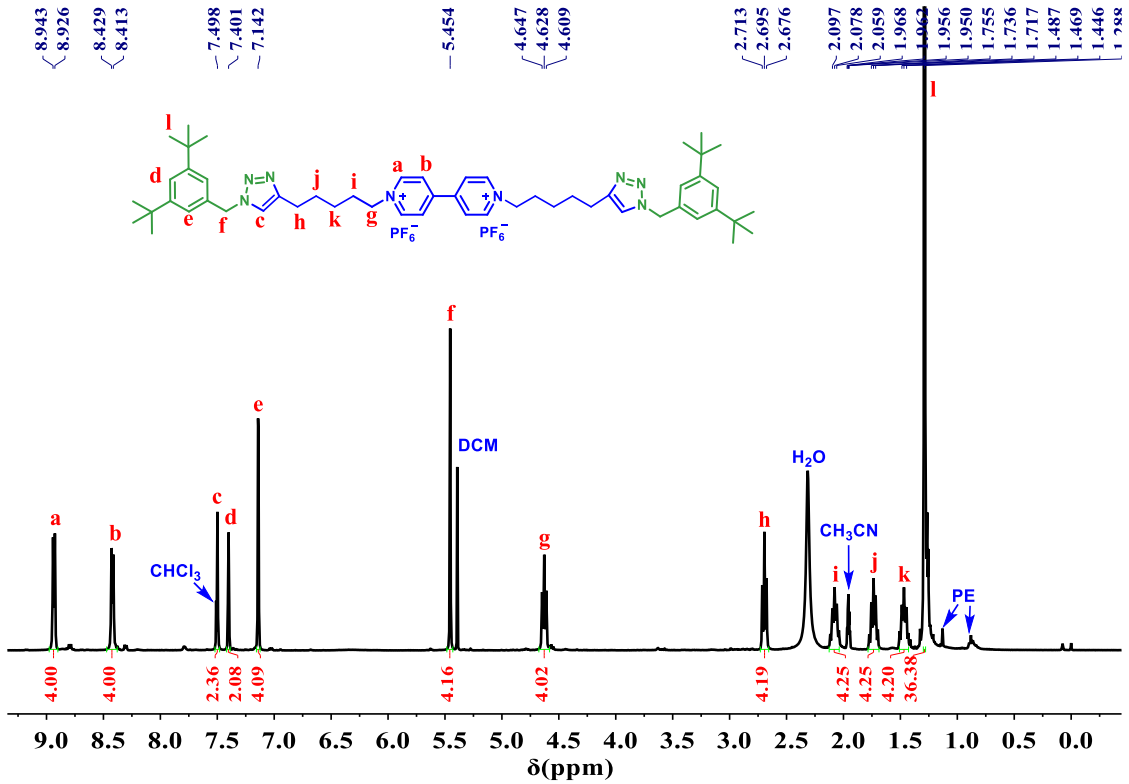

Figure S3. ^{1}H NMR spectrum of **S5** (400 MHz, $CDCl_3/CD_3CN$, 1:1, v/v, 298 K, 20 mM)

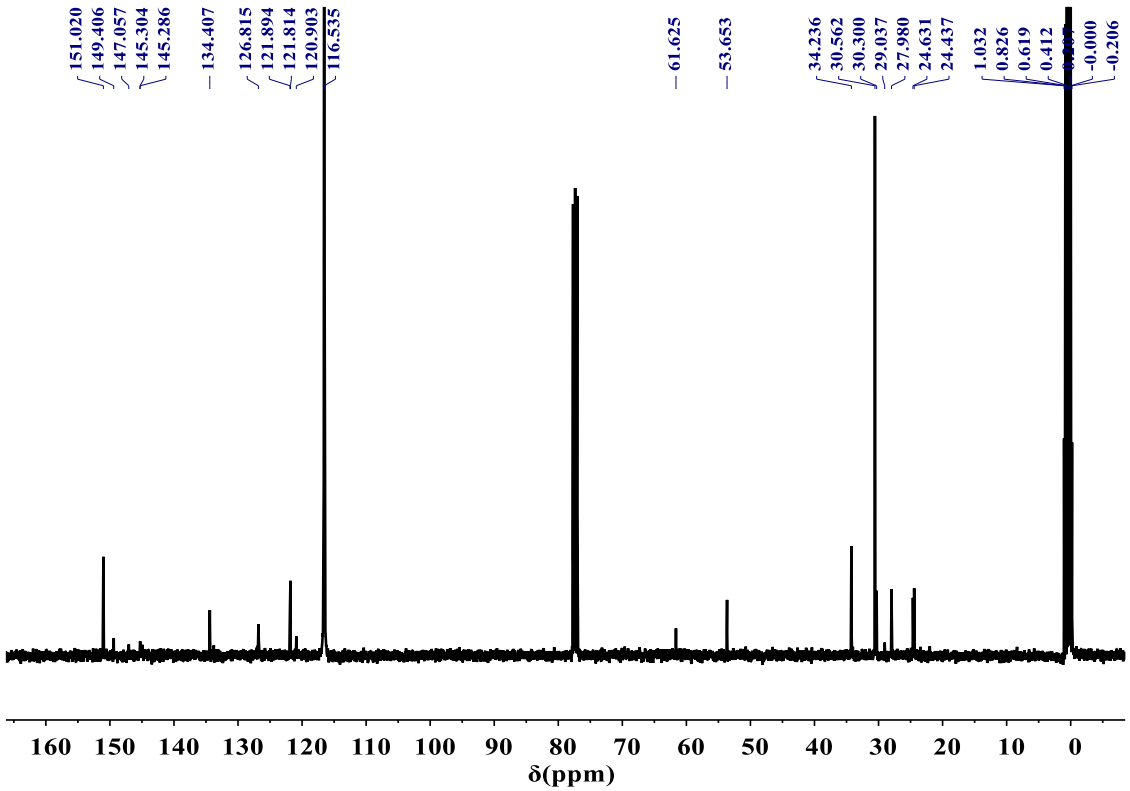

Figure S4 ^{13}C NMR spectrum of **S5** (100 MHz, $CDCl_3/CD_3CN$, 1:1, v/v, 298 K, 20 mM).

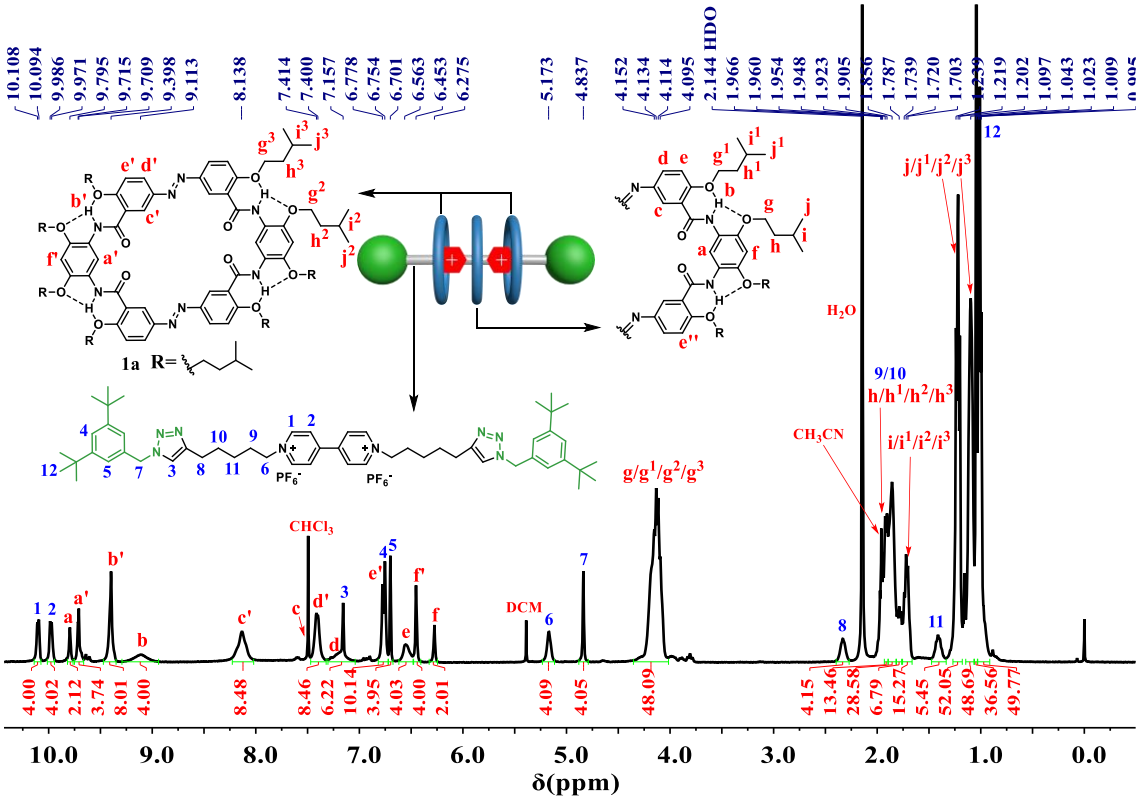

Figure S5. ^{1}H NMR spectrum of **[4]R** (400 MHz, $CDCl_3/CD_3CN$, 1:1, v/v, 298 K, 10 mM)

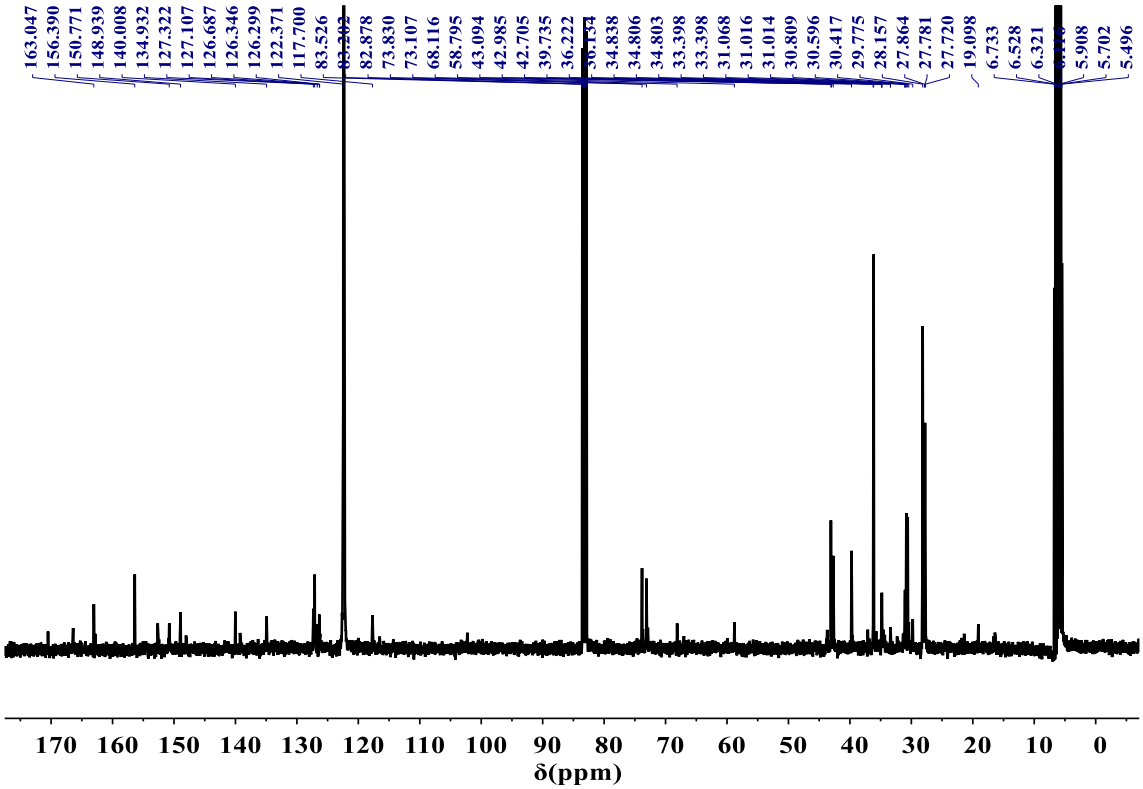

Figure S6 ^{13}C NMR spectrum of **[4]R** (100 MHz, $CDCl_3/CD_3CN$, 1:1, v/v, 298 K, 10 mM).

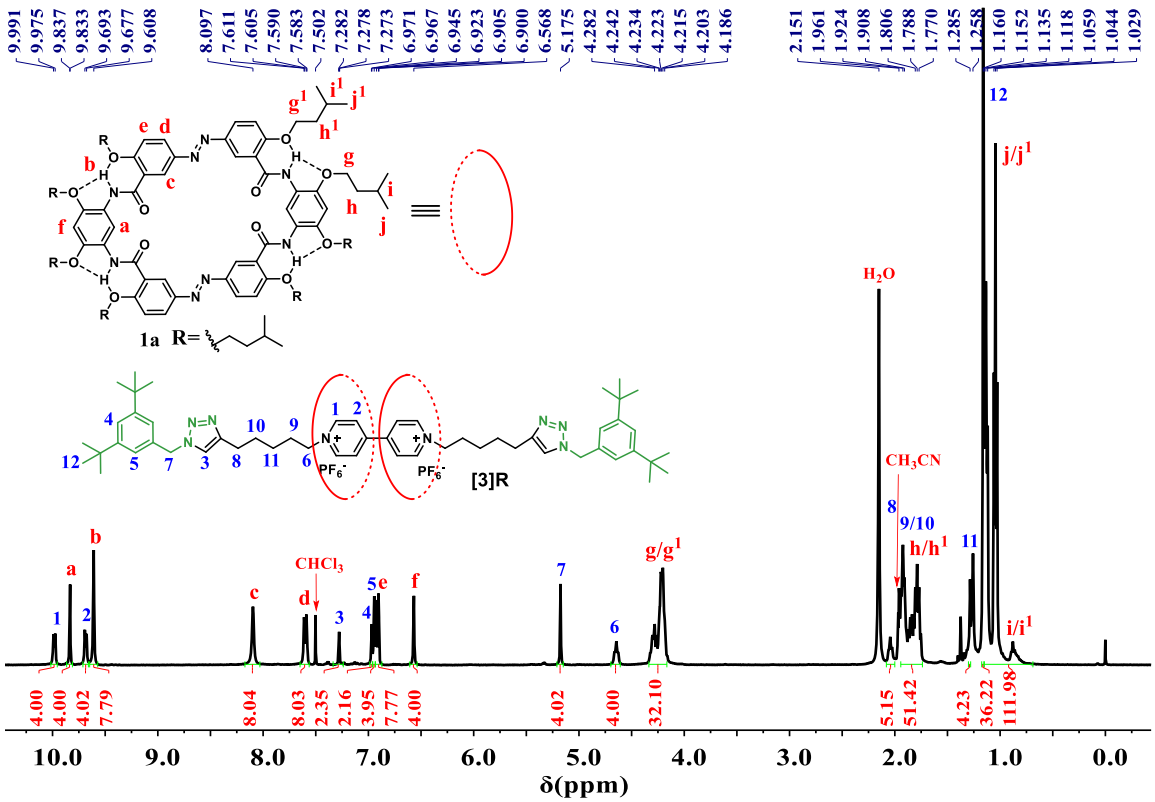

Figure S7. ^{1}H NMR spectrum of **[3]R** (400 MHz, $CDCl_3/CD_3CN$, 1:1, v/v, 298 K, 15 mM)

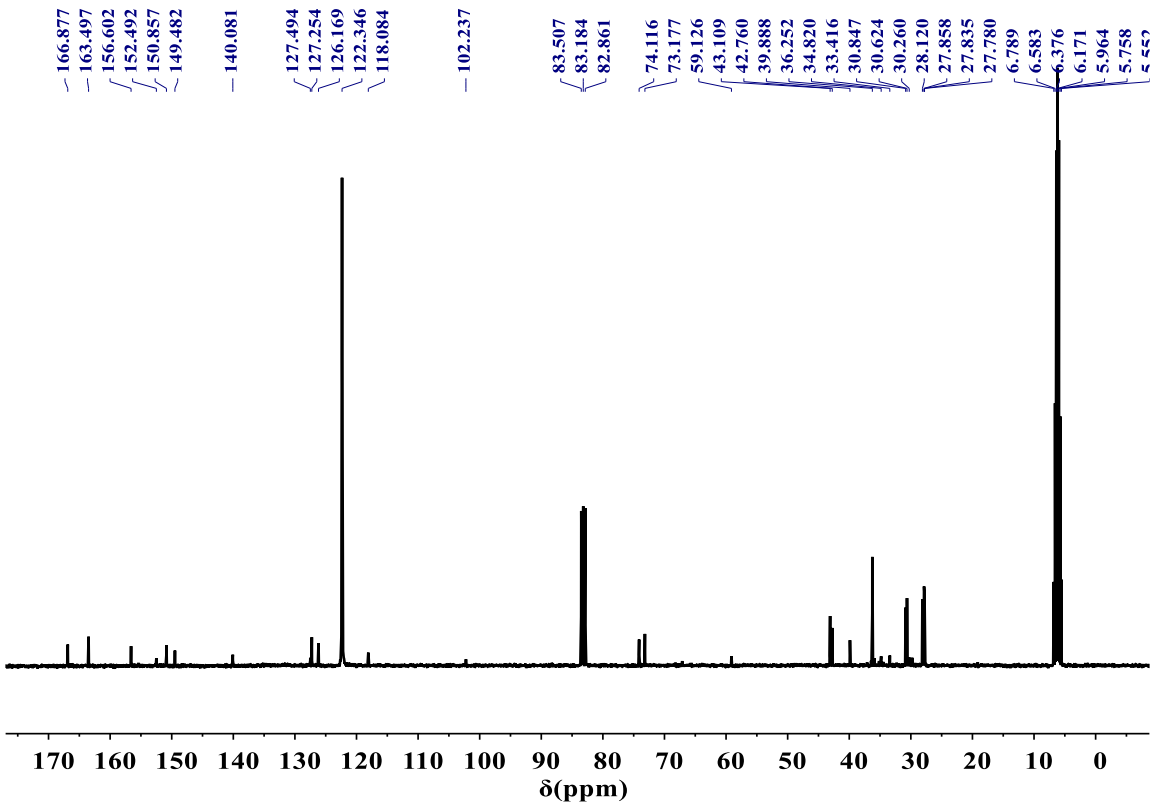

Figure S8 ^{13}C NMR spectrum of **[3]R** (100 MHz, $CDCl_3$/CD_3CN, 1:1, v/v, 298 K, 15 mM).

3.2 HRESI-MS Spectra of Novel Compounds

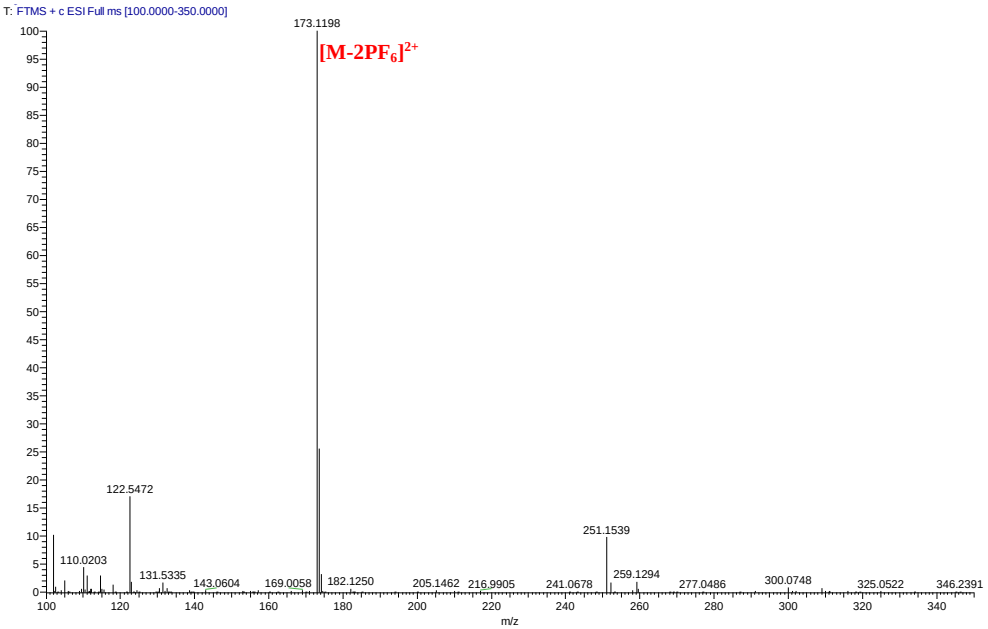

Figure S9 HRESI-MS spectrum of **G2**.

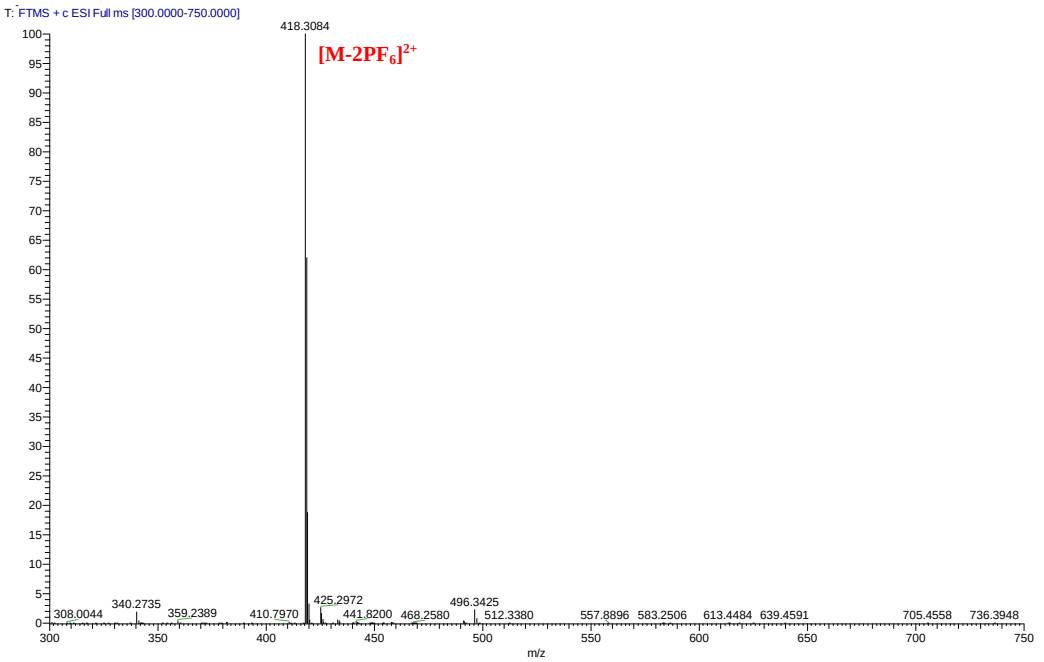

Figure S10 HRESI-MS spectrum of **S5**.

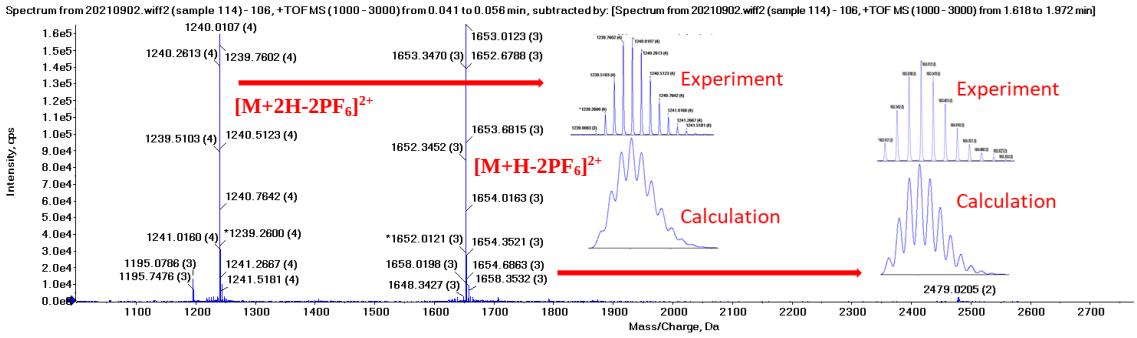

Figure S11 HRESI-MS spectrum of **[4]R**.

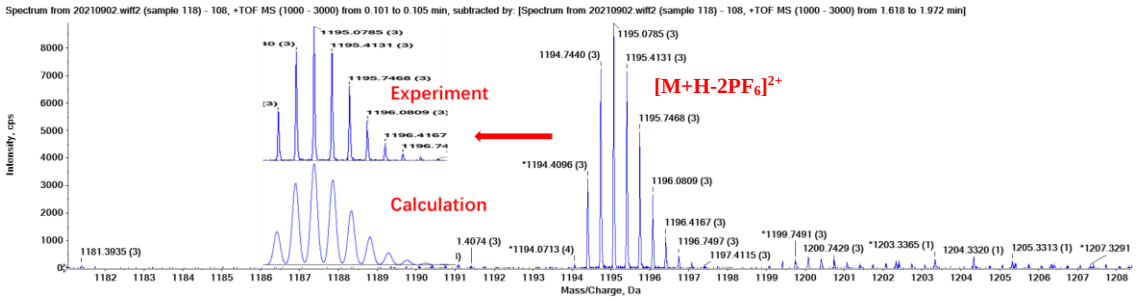

Figure S12 HRESI-MS spectrum of **[3]R**.

4. Host-Guest Complexation of 1a and G1

4.1 NMR Spectra of Complexation

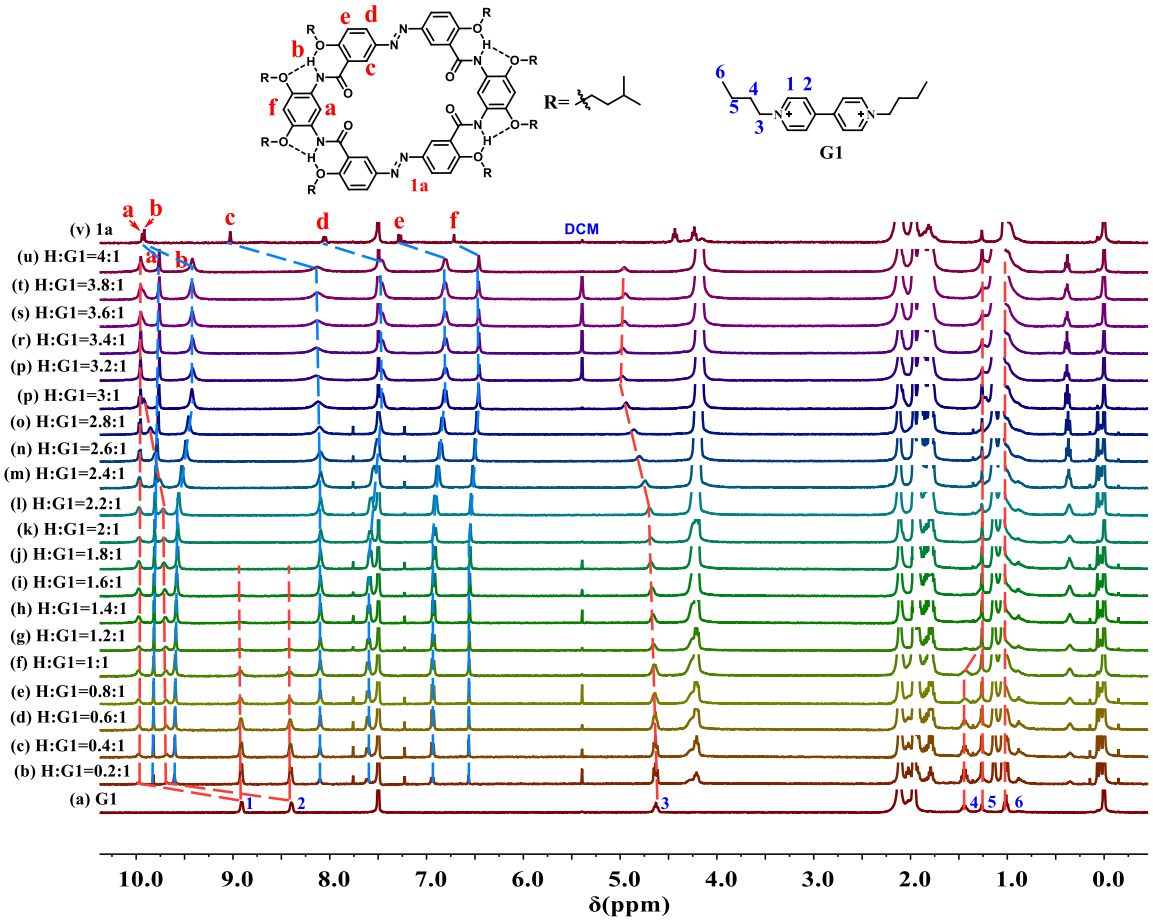

Figure S13 ^{1}H NMR spectra ($CDCl_3/CD_3CN$, 1:1, v/v, 400 MHz, 298 K) of **G1** upon addition of different equiv of **1a** ([**G1**]= 1.0 × 10^{-3} M, [**1a**]/[**G1**]= 0 – 4 eq). (a) 0.0 eq, (b) 0.2 eq, (c) 0.4 eq, (d) 0.6 eq, (e) 0.8 eq, (f) 1.0 eq, (g) 1.2 eq, (h) 1.4 eq, (i) 1.6 eq, (j) 1.8 eq, (k) 2.0 eq, (l) 2.2 eq, (m) 2.4 eq, (n) 2.6 eq, (o) 2.8 mM eq, (p) 3.0 eq, (q) 3.2 eq, (r) 3.4 eq, (s) 3.6 eq, (t) 3.8 eq, (u) 4.0 eq, and (v) only **1a**.

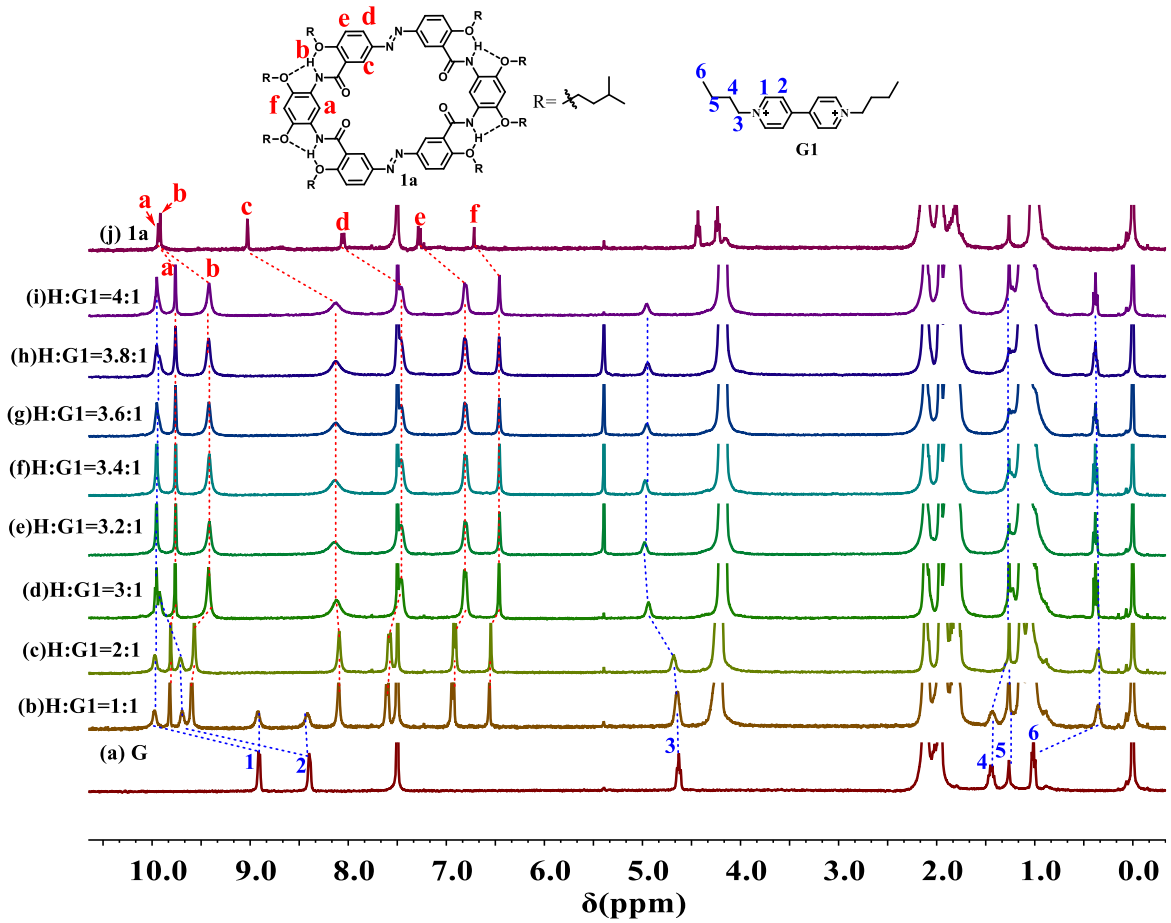

Figure S14 ^{1}H NMR spectra ($CDCl_3/CD_3CN$, 1:1, v/v, 400 MHz, 298 K) of **G1** upon addition of different equiv of **1a** ([**G1**]= 1.0 × 10^{-3} M, [**1a**]/[**G1**]= 0 – 4 eq). (a) 0.0 eq, (b) 1.0 eq, (c) 2.0 eq, (d) 3.0 eq, (e) 3.2 eq, (f) 3.4 eq, (g) 3.6 eq, (h) 3.8 eq, (i) 4.0 eq, and (j) only **1a**.

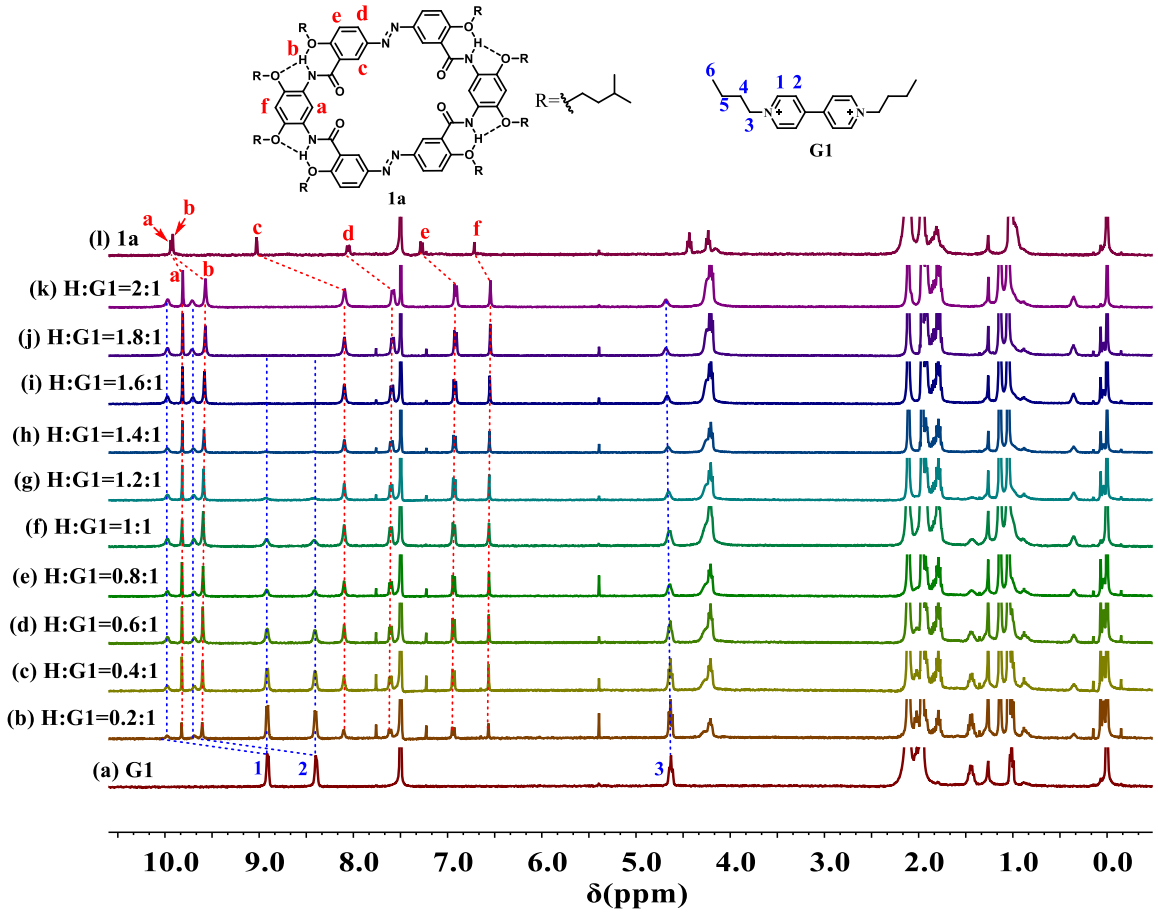

Figure S15 ^{1}H NMR spectra ($CDCl_3/CD_3CN$, 1:1, v/v, 400 MHz, 298 K) of **G1** upon addition of different equiv of **1a** ([**G1**]= 1.0×10^{-3} M, [**1a**]/[**G1**]= 0 – 4 eq). (a) 0.0 eq, (b) 0.2 eq, (c) 0.4 eq, (d) 0.6 eq, (e) 0.8 eq, (f) 1.0 eq, (g) 1.2 eq, (h) 1.4 eq, (i) 1.6 eq, (j) 1.8 eq, (k) 2.0 eq, and (l) only **1a**.

4.2 HRESI-MS Spectra of Complexes

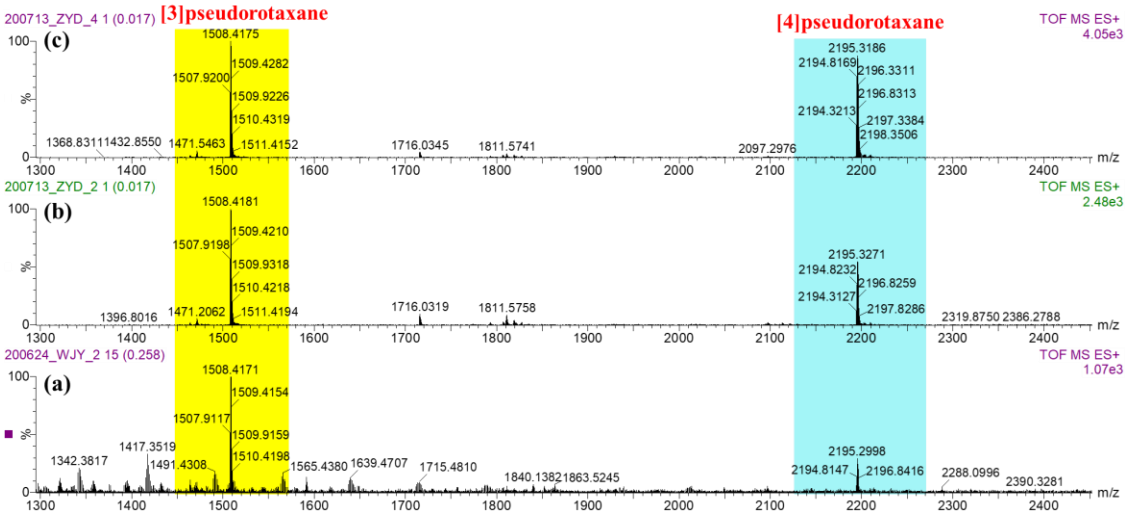

Figure S16 Partial HRESI-MS spectrum of complex **1a** ⊃ **G1**. (a) **1a** : **G1** = 2:1, (b) **1a** : **G1** = 3:1, (c) **1a** : **G1** = 4:1.

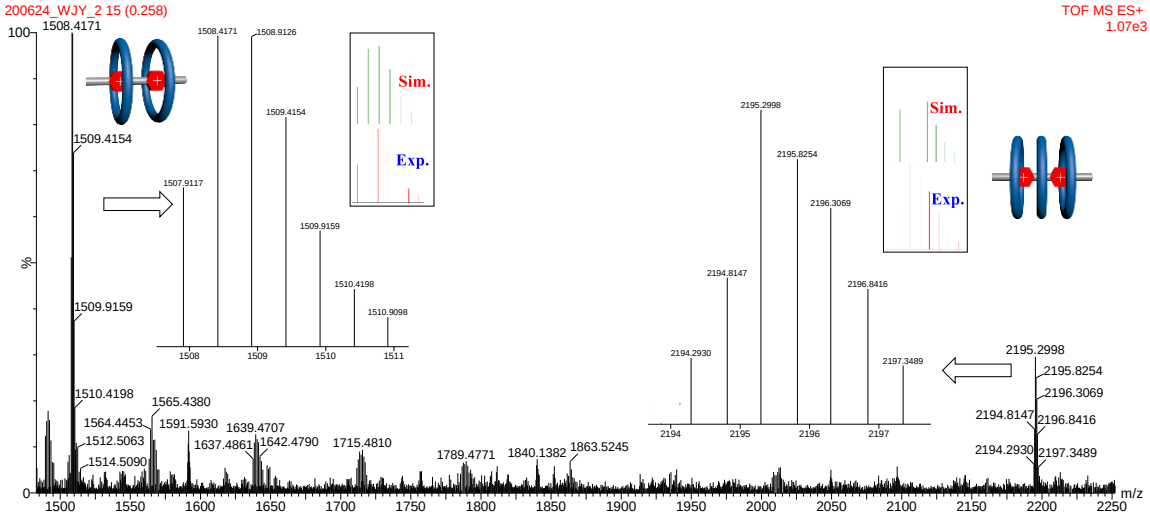

Figure S17 Partial HRESI-MS spectrum of complex **1a** ⊃ **G1** (**1a** : **G1** = 2:1)

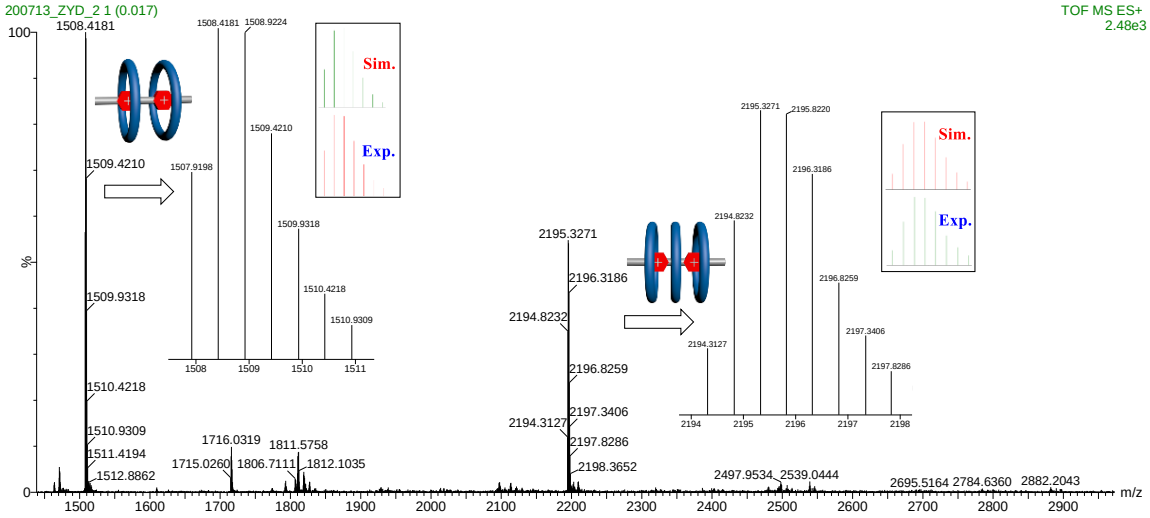

Figure S18 Partial HRESI-MS spectrum of complex **1a** ⊃ **G1** (**1a** : **G1** = 3:1)

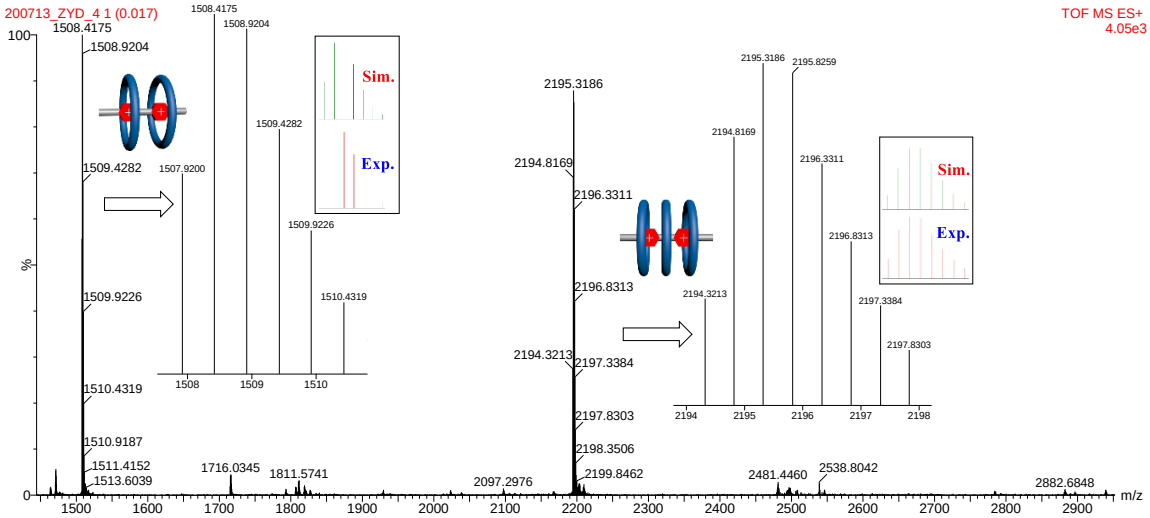

Figure S19 Partial HRESI-MS spectrum of complex **1a** ⊃ **G1** (**1a** : **G1** = 4:1)

4.3 Job Plots of Host-Guest Complexes

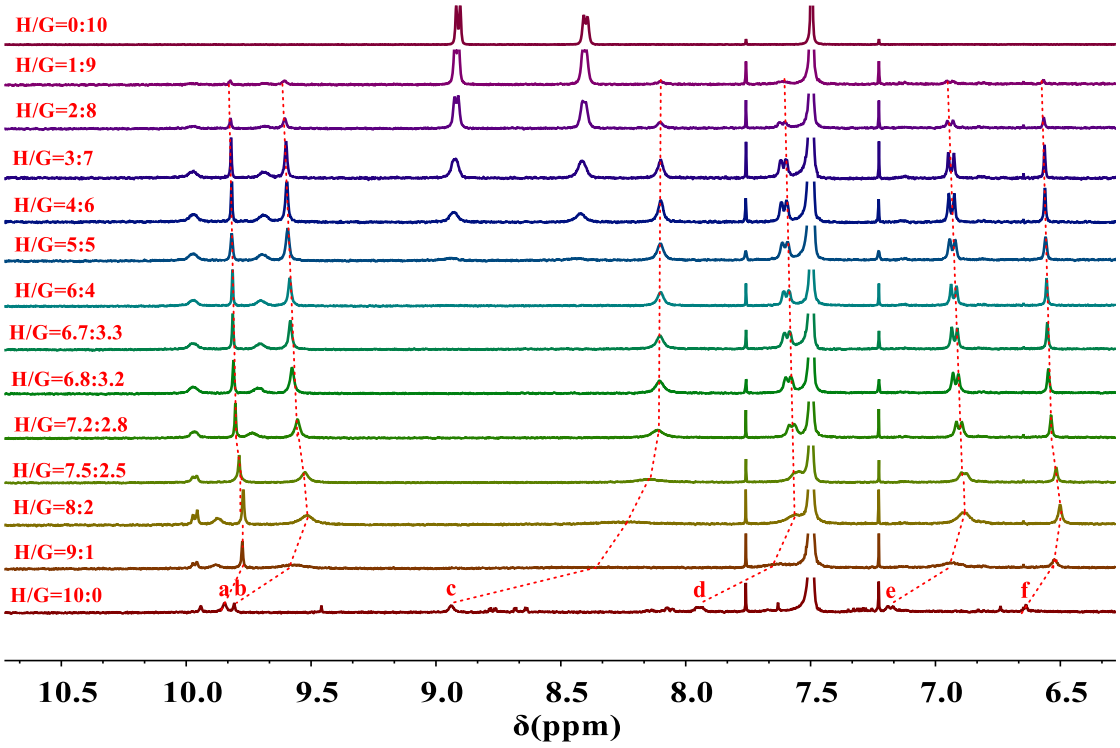

Figure S20 Partial stacked ^{1}H NMR spectra (400 MHz, $CDCl_3/CD_3CN$, 1:1, v/v, 298K) of **1b** ⊃ **G1** in the presence of the different ratio of **1a** and **G1** at a fixed total concentration of 1.0 mM.

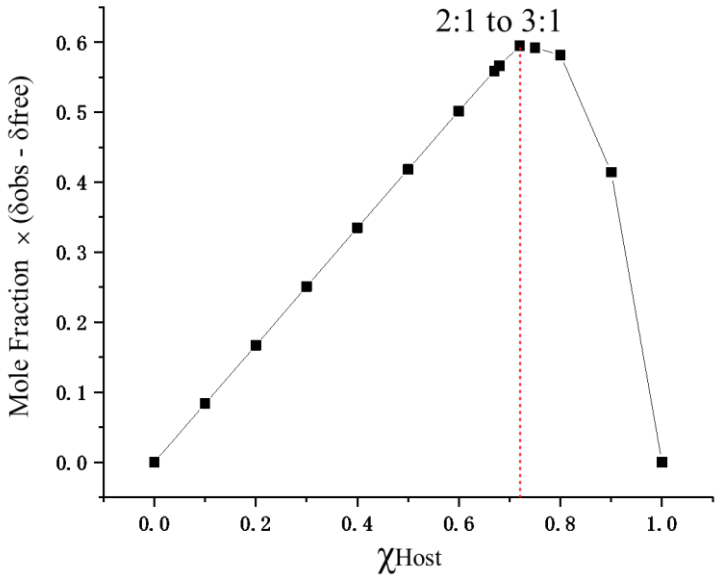

Figure S21 Job plot showing a peak maximum was reached around 0.72 corresponding to the formation of a 2:1 and 3:1 host-guest complex between **1a** and **G1**.

4.4 Determination of the Stoichiometries and Binding Constants

The binding constants between **1a** and **G1** were obtained by ITC technique. With the Multiple Sites to fit the binding constants, 2:1 binding mode was obtained.

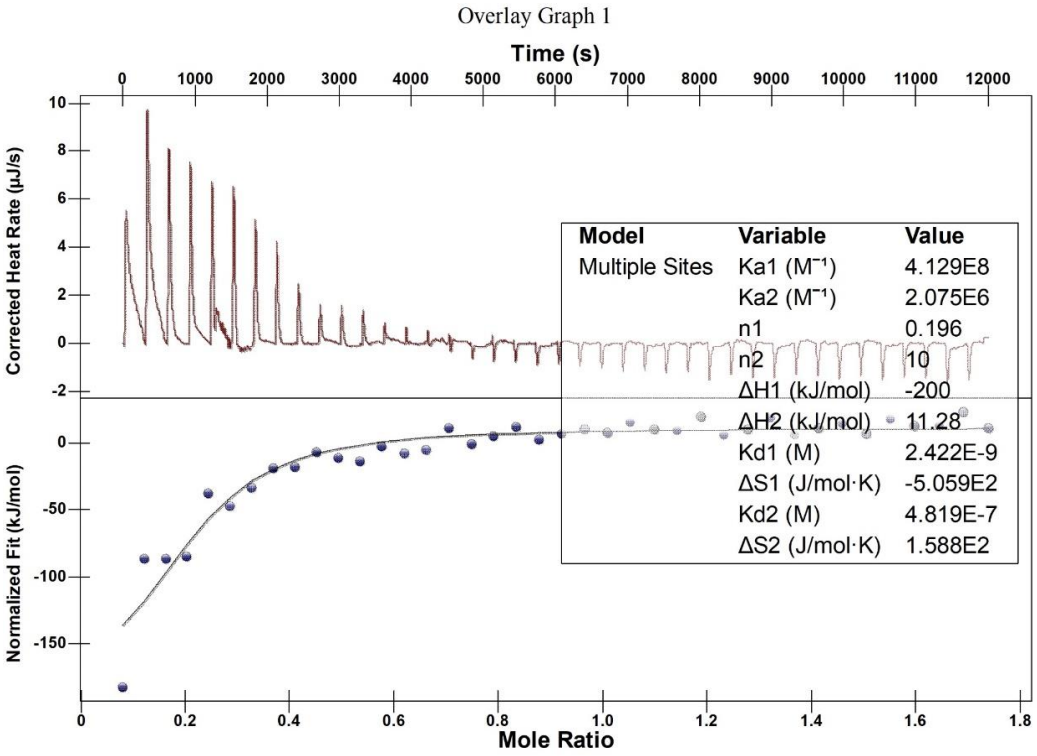

Figure S22 Determination of the association constant of **1a** (50 μM) and **G1** (0.5 mM) in $CHCl_3/CH_3CN$ (1:1, v/v) by ITC.

5. 2D NOESY Spectra of Rotaxane

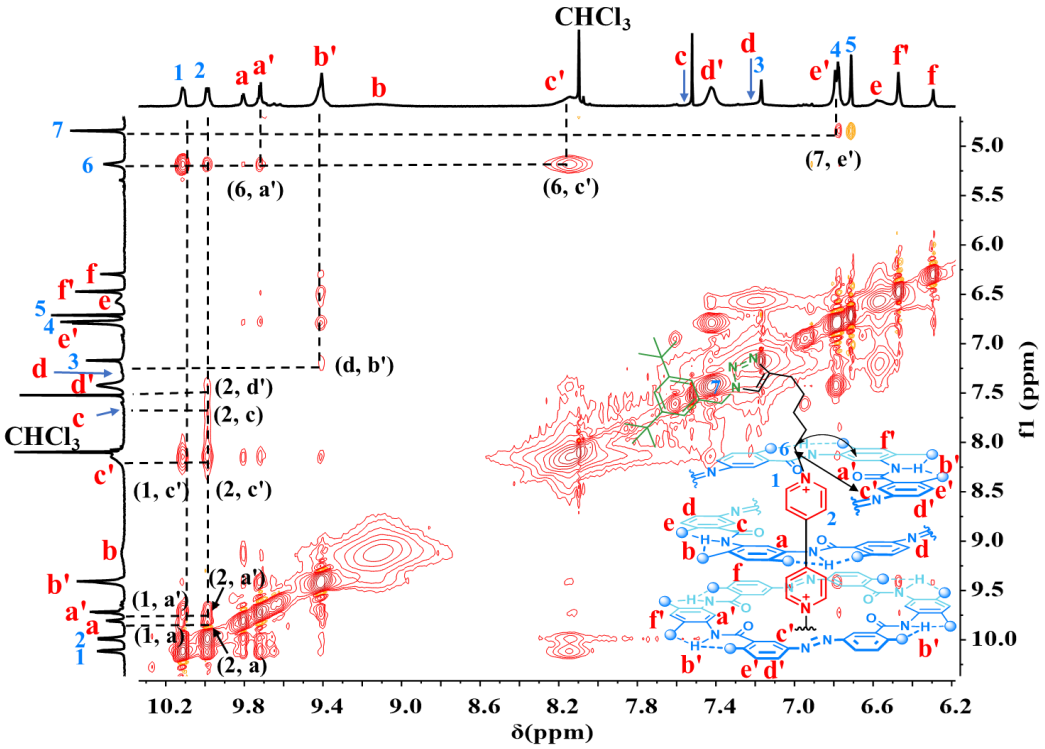

Figure S23 Expanded 2D NOESY spectrum of **[4]R**. (600 MHz, $CDCl_3/CD_3CN$, 1:1, v/v, 298 K , 10 mM, mixing time = 0.4 s)

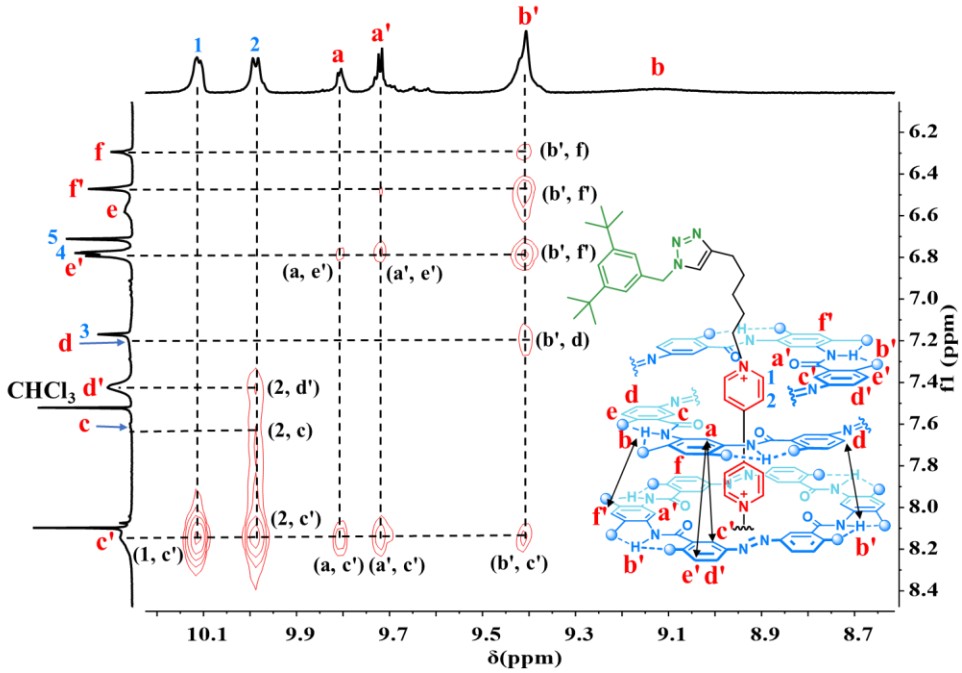

Figure S24 Expanded 2D NOESY spectrum of **[4]R** (600 MHz, $CDCl_3/CD_3CN$, 1:1, v/v, 298 K , 10 mM, mixing time = 0.4 s), indicating the interaction of **1a**.

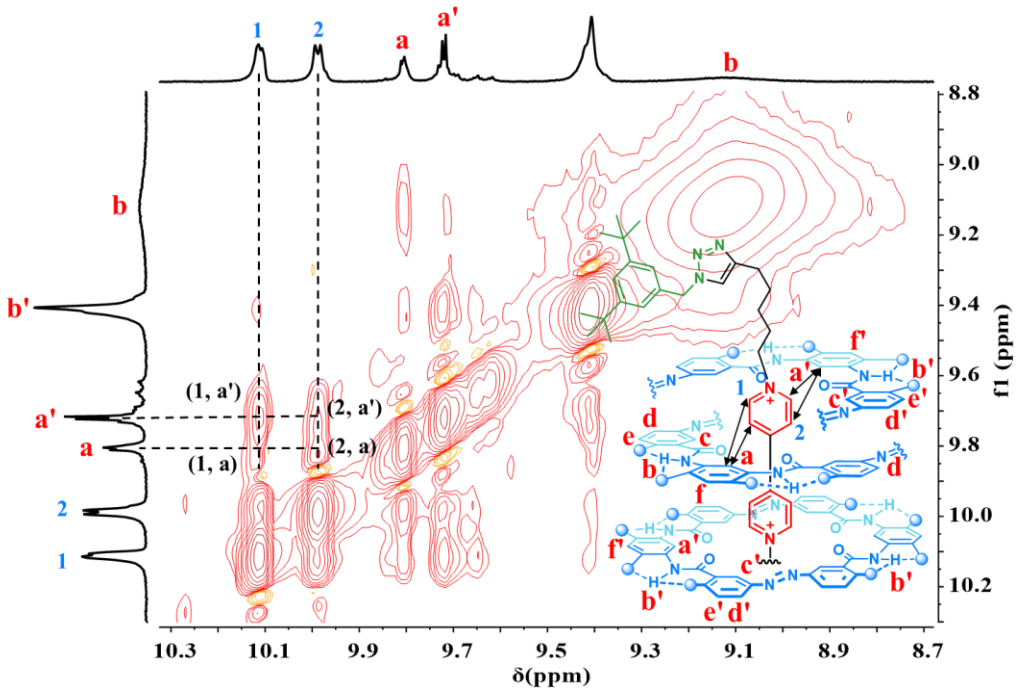

Figure S25 Expanded 2D NOESY spectrum of **[4]R** (600 MHz, $CDCl_3/CD_3CN$, 1:1, v/v, 298 K , 10 mM, mixing time = 0.4 s), indicating the interaction between **1a** and **Axle**.

6. X-ray Single Crystal Structures

Table S1 Crystallographic data and structure refinement for [4]pseudorotaxane **G1⊂1a$_3$**

Identification code	1
CCDC No.	2111239
Empirical formula	$C_{266}H_{366}Cl_8F_{12}N_{26}O_{36}P_2$
Formula weight	5077.37
Temperature/K	150.15
Crystal system	triclinic
Space group	P-1
a/Å	18.4426(7)
b/Å	19.7321(7)
c/Å	20.3347(9)
α/°	91.639(3)
β/°	93.853(3)

γ/°	114.363(4)
Volume/Å^3	6712.9(5)
Z	1
ρ_{calc}g/cm^3	1.256
μ/mm^{-1}	1.538
F(000)	2706.0
Crystal size/mm^3	0.13 × 0.11 × 0.1
Radiation	CuKα (λ = 1.54184)
2Θ range for data collection/°	6.554 to 132.016
Index ranges	-21 ≤ h ≤ 20, -17 ≤ k ≤ 23, -24 ≤ l ≤ 23
Reflections collected	37631
Independent reflections	23038 [R_{int} = 0.0267, R_{sigma} = 0.0349]
Data/restraints/parameters	23038/150/1723
Goodness-of-fit on F^2	1.028
Final R indexes [I>=2σ (I)]	R_1 = 0.0661, wR_2 = 0.1739
Final R indexes [all data]	R_1 = 0.0840, wR_2 = 0.1928
Largest diff. peak/hole / e Å^{-3}	1.20/-1.07

Table S2 N$^+$···O interaction in the crystal structure of [4]pseudorotaxane **G1⊂1a$_3$**

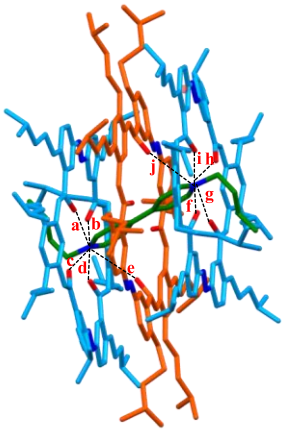

No. of N$^+$···O interaction	N$^+$···O / Å	No. of N$^+$···O interaction	N$^+$···O / Å
a	4.199	b	3.802
c	3.660	d	4.186
e	3.620	f	3.802
g	4.199	h	3.660
i	4.186	j	3.620

Table S3 C-H···O hydrogen bonds in the crystal structure of [4]pseudorotaxane **G1⊂1a$_3$**

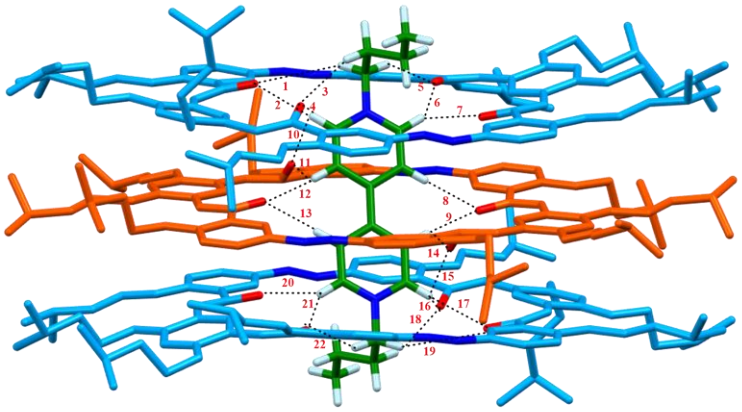

No. of C-H···O interaction	H···O / Å C-H···O angles	No. of C-H···O interaction	C-H···O / Å C-H···O angles
1	3.218 (146.63°)	2	2.494 (141.49°)
3	2.703 (148.38°)	4	2.574 (142.98°)
5	2.483 (142.10°)	6	2.498 (152.75°)
7	2.370 (171.46°)	8	2.276 (135.00°)
9	2.234 (170.98°)	10	2.719 (164.95°)
11	2.788 (145.04°)	12	2.234 (170.98°)
13	2.276 (135.00°)	14	2.788 (145.04°)
15	2.719 (164.95°)	16	2.574 (142.98°)
17	2.494 (141.49°)	18	2.703 (141.49°)
19	3.281 (146.63°)	20	2.370 (171.46°)
21	2.498 (152.75°)	22	2.483 (142.10°)

Table S4 π-π stacking in the crystal structure of [4]pseudorotaxane **G1⊂1a$_3$**

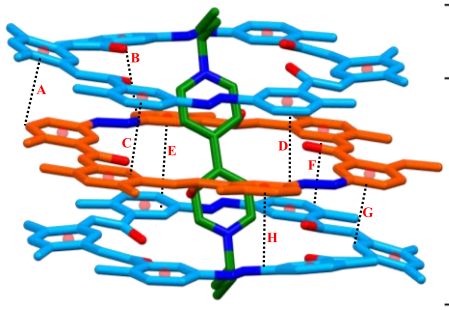

No. of π-π stacking	Centroid to plane / Å	No. of π-π stacking	Centroid to plane / Å
A	3.564	B	3.230
C	3.422	D	3.544
E	3.063	F	3.487
G	3.272	H	3.463

7 Conformational Optimization of Rotaxane by xTB

In order to gain a better understanding of the geometrical superstructure of the **[4]R**, xTB methods have been carried out based on the crystal structure of pseudo[4]rotaxane. Figure S26 show the energy minimization structures of the rotaxane.[4]

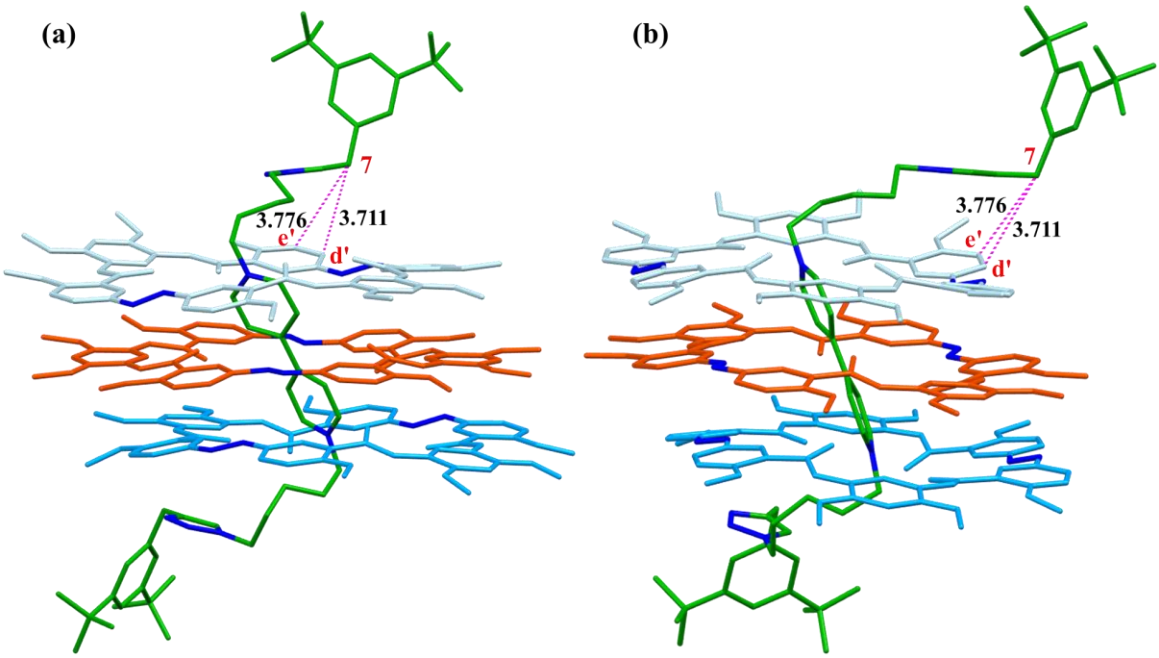

Figure S26 Optimized superstructure of the **[4]R** from xTB methods. (a-b) Capped-stick representations of different views of the **[4]R**.

8. Determination of Rotaxanes Yields

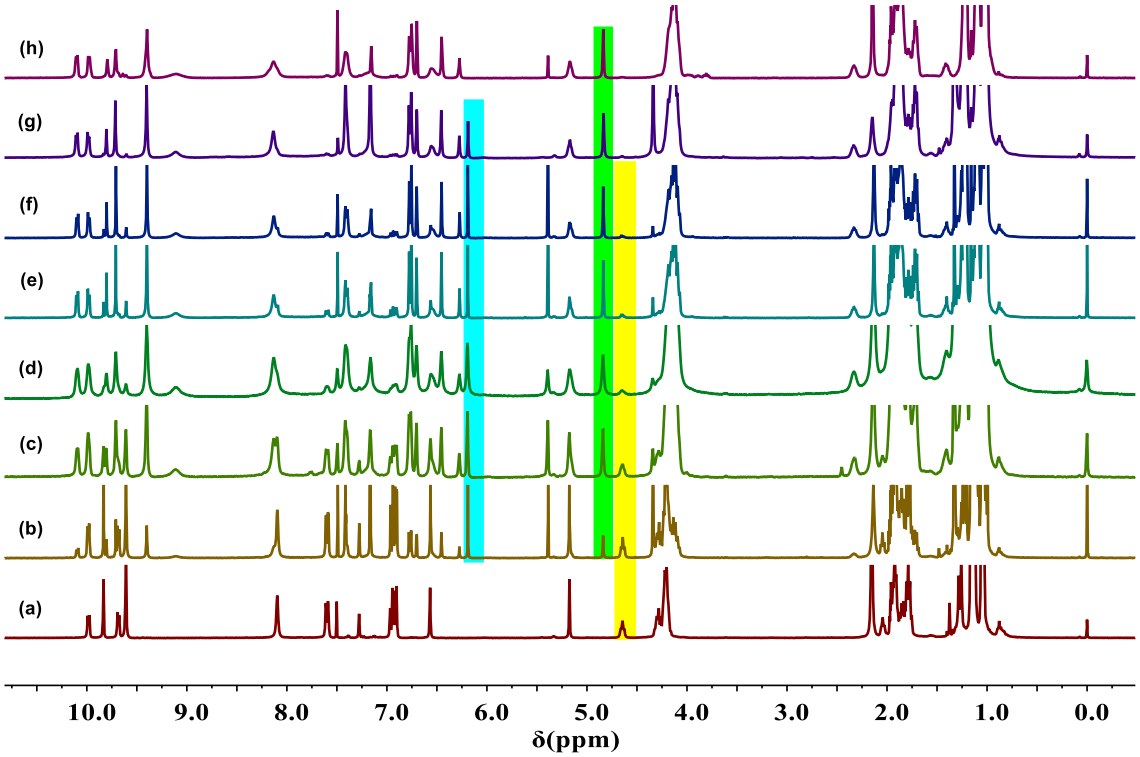

Figure S27 Stacked ^{1}H NMR spectra of rotaxanes with different ratios of **1a** and **G2**: (a) **[3]R** (yellow), (b) **1a**:**G2** = 2:1, (c) **1a**:**G2** = 3:1, (d) **1a**:**G2** = 4:1, (e) **1a**:**G2** = 5:1, (f) **1a**:**G2** = 6:1, (g) **1a**:**G2** = 10:1, (h) **[4]R** (green), internal standard(bule). (400 MHz, $CDCl_3/CD_3CN$, 1:1, v/v, 298 K).

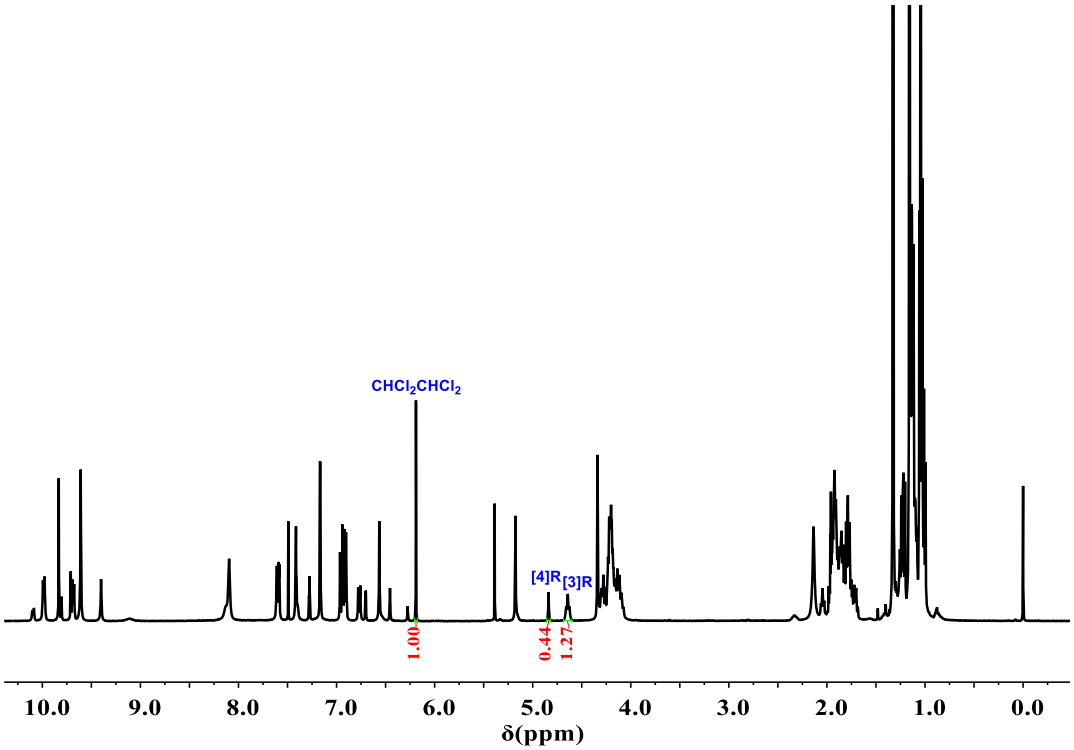

Figure S28 ^{1}H NMR spectrum of reaction mixture of rotaxanes under the condition of **1a**:**G2** = 2:1. (400 MHz, $CDCl_3$/CD_3CN, 1:1, v/v, 298 K).

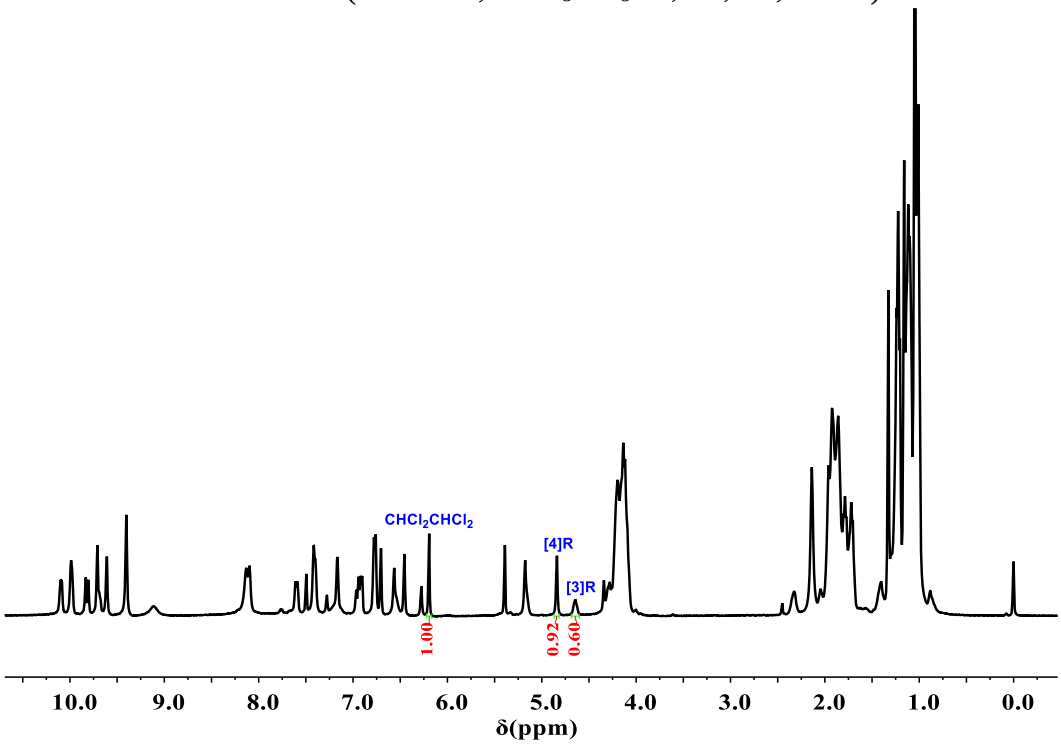

Figure S29 ^{1}H NMR spectrum of reaction mixture of rotaxanes under the condition of **1a**:**G2** = 3:1. (400 MHz, $CDCl_3$/CD_3CN, 1:1, v/v, 298 K).

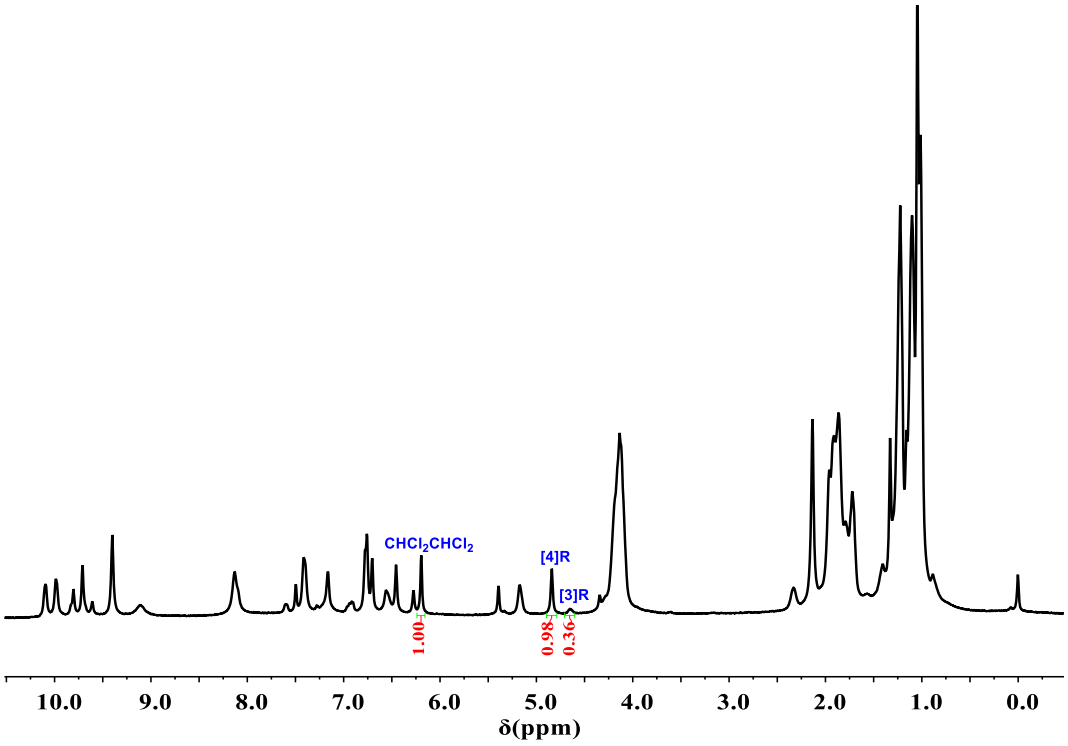

Figure S30 ^{1}H NMR spectrum of reaction mixture of rotaxanes under the condition of **1a**:**G2** = 4:1. (400 MHz, $CDCl_3$/CD_3CN, 1:1, v/v, 298 K).

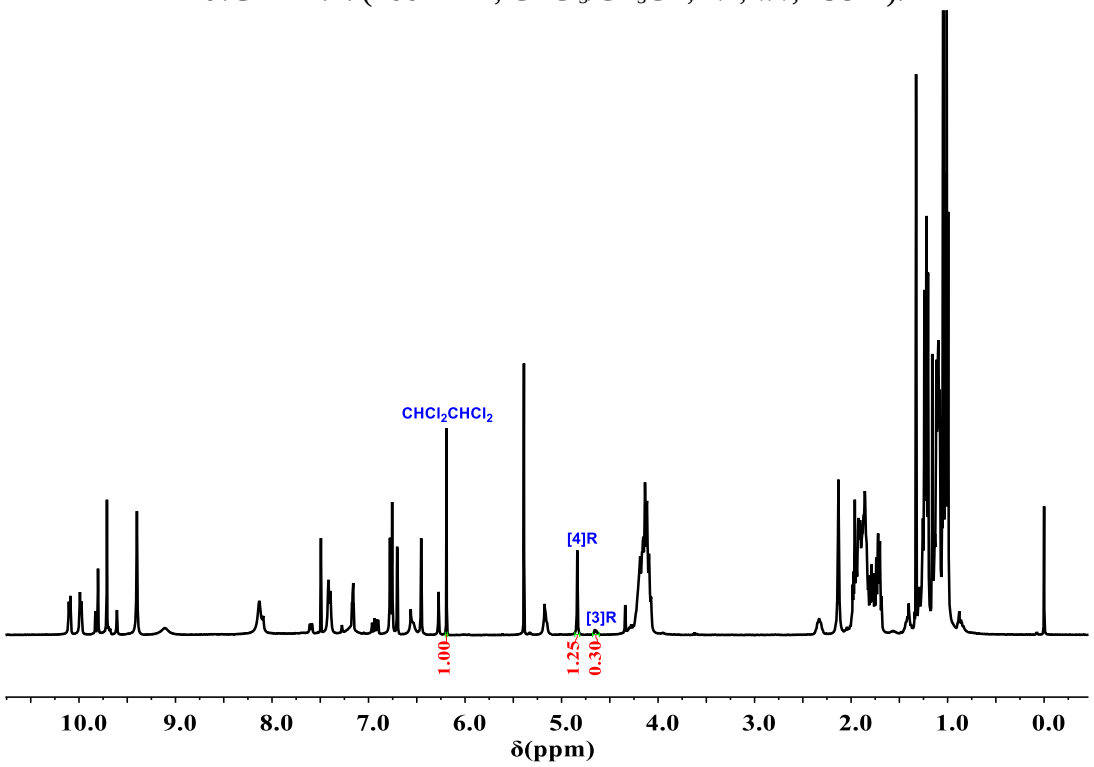

Figure S31 ^{1}H NMR spectrum of reaction mixture of rotaxanes under the condition of **1a**:**G2** = 5:1. (400 MHz, $CDCl_3$/CD_3CN, 1:1, v/v, 298 K).

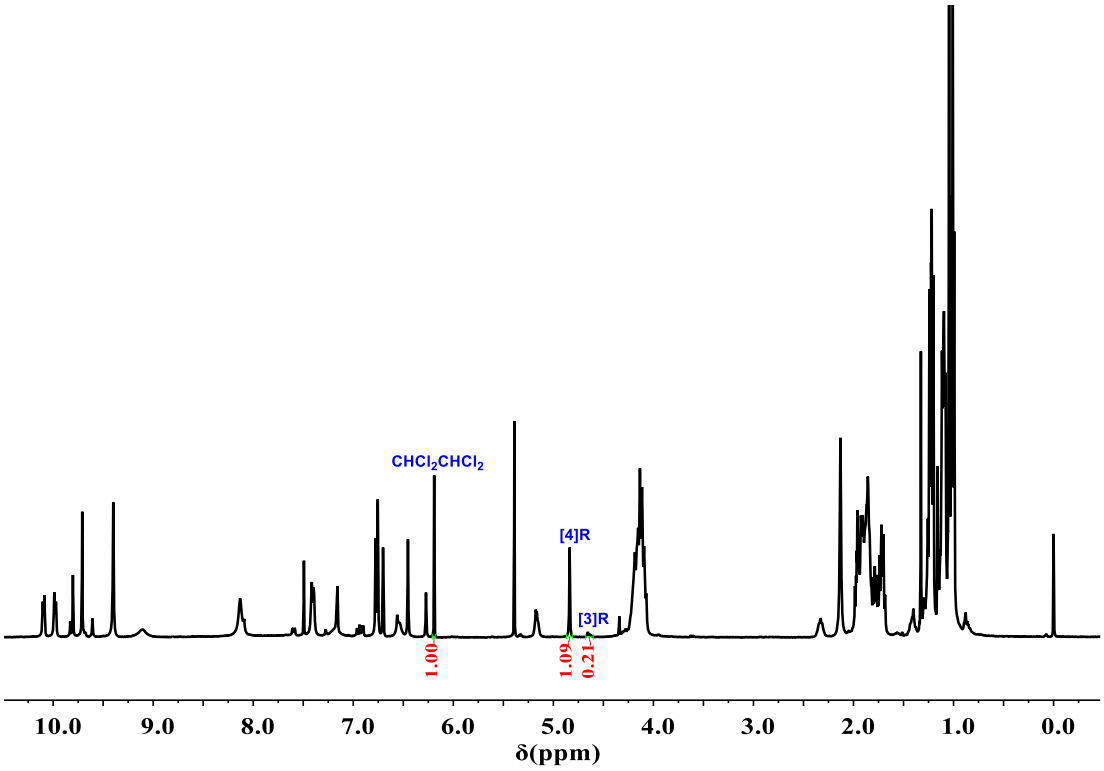

Figure S32 ^{1}H NMR spectrum of reaction mixture of rotaxanes under the condition of **1a**:**G2** = 6:1. (400 MHz, $CDCl_3/CD_3CN$, 1:1, v/v, 298 K).

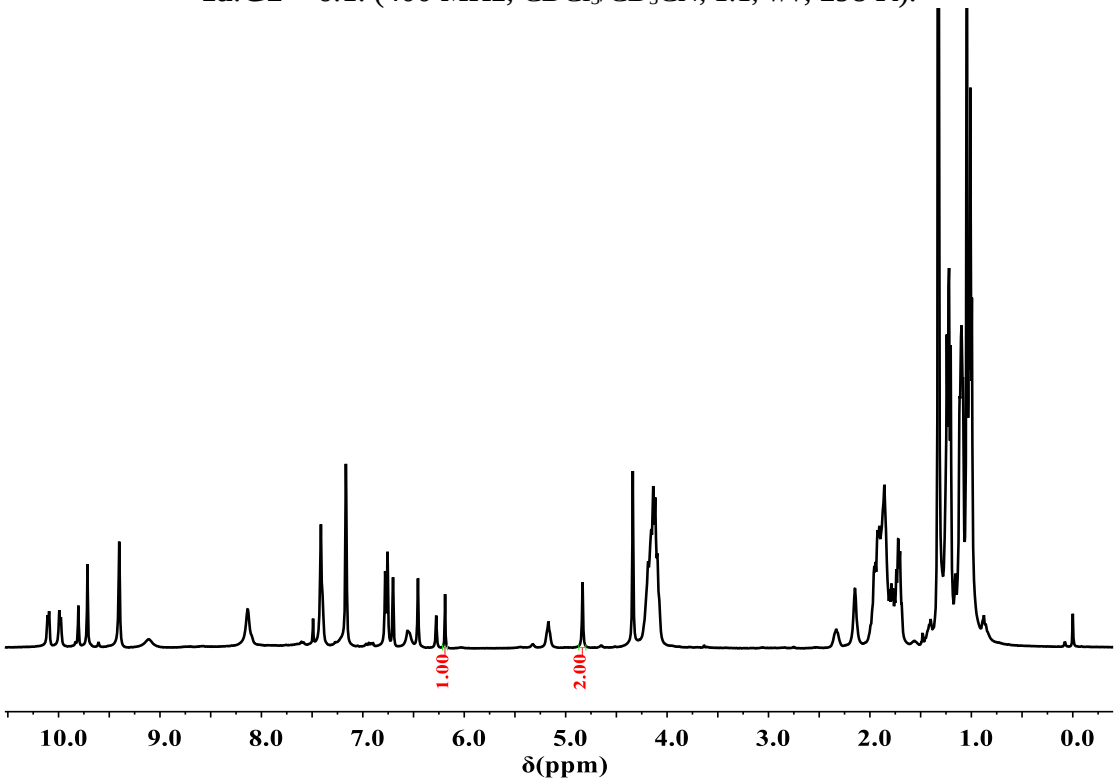

Figure S33 ^{1}H NMR spectrum of reaction mixture of rotaxanes under the condition of **1a**:**G2** = 10:1. (400 MHz, $CDCl_3/CD_3CN$, 1:1, v/v, 298 K).

References

[1] X. W. Li, X. Y. Yuan, P. C. Deng, L. X. Chen, Y. Ren, C. Y. Wang, L. X. Wu, W. Feng, B. Gong and L. H. Yuan, *Chem. Sci*., **2017**, 8, 2091-2100.

[2] S. Su, Z. Yang, H. Y. Gao, H. Y. Yang, S. B. Zhu, Z. X. An, J. J. Wang, Q. Li, S. Chandarlapaty, H. T. Deng, W. Wu and Y. Rao, *J. Med. Chem*., **2019**, 62, 7575-7582.

[3] Z. C. Ye, Z. Y. Yang, L. Wang, L. X. Chen, Y. M. Cai, P. C. Deng, W. Feng, X. P. Li and L. H. Yuan, *Angew. Chem. Int. Ed*., 2019, **58**, 12519-12523.

[4] J. Seibert, C. Bannwarth and S. Grimme, *J. Am. Chem. Soc*., 2017, **139**, 11682-11685.